Developmental Biology 480 (2021) 62–68

Contents lists available at ScienceDirect

Developmental Biology

journal homepage: www.elsevier.com/locate/developmentalbiology

# Protein fucosylation is required for Notch dependent vascular integrity in zebrafish

Gerissa Fowler [a], Danielle V. French [a], April Rose [a], Paige Squires [a], Catarina Aniceto da Silva [a], Shinya Ohata [b], Hitoshi Okamoto [c], Curtis R. French [a,*]

[a] Division of Biomedical Sciences, Faculty of Medicine, Memorial University of Newfoundland, St. John's, NL, Canada
[b] Molecular Cell Biology Laboratory, Research Institute of Pharmaceutical Sciences, Faculty of Pharmacy, Musashino University, Tokyo, Japan
[c] Laboratory for Neural Circuit Dynamics of Decision-making, RIKEN Center for Brain Science, Saitama, Japan

ARTICLE INFO

*Keywords:*
*gmds*
Notch signaling
Fucosylation
Hemorrhage
Mural cell
Endothelial cell
Zebrafish

ABSTRACT

The onset of circulation in a developing embryo requires intact blood vessels to prevent hemorrhage. The development of endothelial cells, and their subsequent recruitment of perivascular mural cells are important processes to establish and maintain vascular integrity. These processes are genetically controlled during development, and mutations that affect endothelial cell specification, pattern formation, or maturation through the addition of mural cells can result in early developmental hemorrhage. We created a strong loss of function allele of the zebrafish *GDP-mannose 4,6 dehydratase* (*gmds*) gene that is required for the *de novo* synthesis of GDP-fucose, and homozygous embryos display cerebral hemorrhages. Our data demonstrate that *gmds* mutants have early defects in vascular patterning with ectopic branches observed at time of hemorrhage. Subsequently, defects in the number of mural cells that line the vasculature are observed. Moreover, activation of Notch signaling rescued hemorrhage phenotypes in *gmds* mutants, highlighting a potential downstream pathway that requires protein fucosylation for vascular integrity. Finally, supplementation with fucose can rescue hemorrhage frequency in *gmds* mutants, demonstrating that synthesis of GDP-fucose via an alternative (salvage) pathway may provide an avenue toward therapeutic correction of phenotypes observed due to defects in *de novo* GDP-fucose synthesis. Together, these data are consistent with a novel role for the *de novo* and salvage protein fucosylation pathways in regulating vascular integrity through a Notch dependent mechanism.

## 1. Introduction

Protein fucosylation is an essential post-translational modification that is required for the function of many signaling pathways. In vertebrates, two complementary pathways are present to produce GDP-fucose, the substrate for protein fucosylation; the *de novo* synthesis pathway whereby GDP-fucose is generated from mannose-based substrates, and the salvage pathway utilizing free cellular fucose. Defects in the ability to produce GDP-fucose or their transfer to proteins or oligosaccharide chains can cause a host of disease states, including leukocyte adhesion deficiency (Cagdas et al., 2014; Sturla et al., 2003, 2005), glaucoma (Cui et al., 2017; Gharahkhani et al., 2014), and cancer (Moriwaki et al., 2009; Wang et al., 2017). As a genome wide association (GWA) study identified single nucleotide polymorphisms (Snps) within the *GMDS* gene (required for *de novo* GDP-fucose synthesis) as associated with stroke risk (French et al., 2014), we assessed whether *gmds* was required for vascular integrity in a zebrafish model system.

Zebrafish make an ideal animal to test for vascular associated phenotypes given their conserved cardiovascular development with humans, optical transparency, and numerous transgenic lines that highlight vascular cell types. Like all vertebrates, zebrafish blood vessels are first formed as endothelial cell tubes that later mature via the addition of mural cells (vascular smooth muscle cells on larger vessels and pericytes on smaller vessels). The specification of endothelial cells and early vasculogenesis requires the function of Vascular Endothelial Growth Factor (VEGF) signalling pathways, with Notch and Hedgehog signalling pathways installing arterial or venous fate early in development (Gore et al., 2012). The addition of mural cells to newly forming vasculature is an essential process to ensure vascular function and stability as they provide contractability, physical support, as well as regulation of blood brain

* Corresponding author. Discipline of Genetics, Faculty of Medicine Memorial University of Newfoundland, 5M327 Craig L. Dobbin Genetics Research Center 300 Prince Philip Drive, St. John's, A1B 3V6, Canada.
*E-mail address:* curtis.french@med.mun.ca (C.R. French).

https://doi.org/10.1016/j.ydbio.2021.08.004
Received 15 February 2021; Received in revised form 10 August 2021; Accepted 11 August 2021
Available online 13 August 2021
0012-1606/© 2021 Elsevier Inc. All rights reserved.

barrier (Armulik et al., 2010; Bahrami and Childs, 2018; Gaengel et al., 2009). As such, vasculature maturation is tightly controlled during development, with signaling pathways such as Notch (Ehling et al., 2013; Wang et al., 2014) and Platelet Derived Growth Factors (PDGF) (Hellberg et al., 2010), and transcription factors such as Foxc1a and Foxc1b (French et al., 2014; Siegenthaler et al., 2013), regulating their recruitment and differentiation. Inhibition of key members of these signaling pathways, or mutation of *foxc1* transcription factors results in cerebral hemorrhage, demonstrating their role in maintaining vascular stability.

Previously, two zebrafish *gmds* mutant strains (*slytherin* and *towhead*) were used to model leukocyte adhesion deficiency and to study motor neuron progenitor migration (Ohata et al., 2009; Song et al., 2010). The *slytherin* mutant exhibited curly tails and abnormal swimming, which were attributed partially to defects in Notch signaling, while the study of *towhead* revealed similar phenotypes but no defects in the Notch signaling pathway. Such discrepancies may be due to the nature of the reported mutated alleles which contain different missense mutations. Neither study reported any vascular phenotypes in these *gmds* mutant strains or identified expression of fucosylation pathway components in key cells and tissues that could contribute to vascular phenotypes.

To this end, we created a new strong loss of function *gmds* allele through CRISPR genome editing and assayed for vascular phenotypes in this strain, as well as the previously reported *towhead* mutant strain and *gmds* morphants. Given the known requirement for Notch receptor fucosylation (Pandey et al., 2019; Takeuchi and Haltiwanger, 2014; Zhou et al., 2008) and the role of this pathway in regulating endothelial cell development (Akil et al., 2021; Lanner et al., 2007; Lawson et al., 2001) and vascular maturation (Naito et al., 2020; Scheppke et al., 2012; Wang et al., 2014), we tested whether defects in Notch signaling drive *gmds* mutant vascular phenotypes. We further assessed whether the fucose salvage pathway can partially compensate for loss of *gmds* and *de novo* GDP -fucose synthesis. Here, we report that mutation of *gmds* in zebrafish results in cerebral hemorrhage, with mutants displaying ectopic vessels branches and defects in mural cell coverage of nascent vessels while providing supporting data for a role of the Notch signaling pathway as a key downstream regulator of these *gmds* vascular-based phenotypes.

## 2. Results and discussion

### 2.1. Mutation or morpholino inhibition of gmds causes cerebral hemorrhage

We created a zebrafish *gmds* mutant model using the CRISPR-Cas9 system resulting in a missense mutation and a one base pair insertion, creating a new in-frame stop codon at the target site in exon 6 of the principal *gmds* transcript (Fig. 1 C, D). The mutant transcripts are targeted for degradation through the nonsense mediated decay pathway (Fig. S1). Homozygous mutants ($gmds^{n1002\ -/-}$) demonstrates cerebral hemorrhaging in the forebrain and midbrain-hindbrain boundary as early as 42 hpf, increasing in frequency until 3 dpf (Fig. 1A and B). By 3

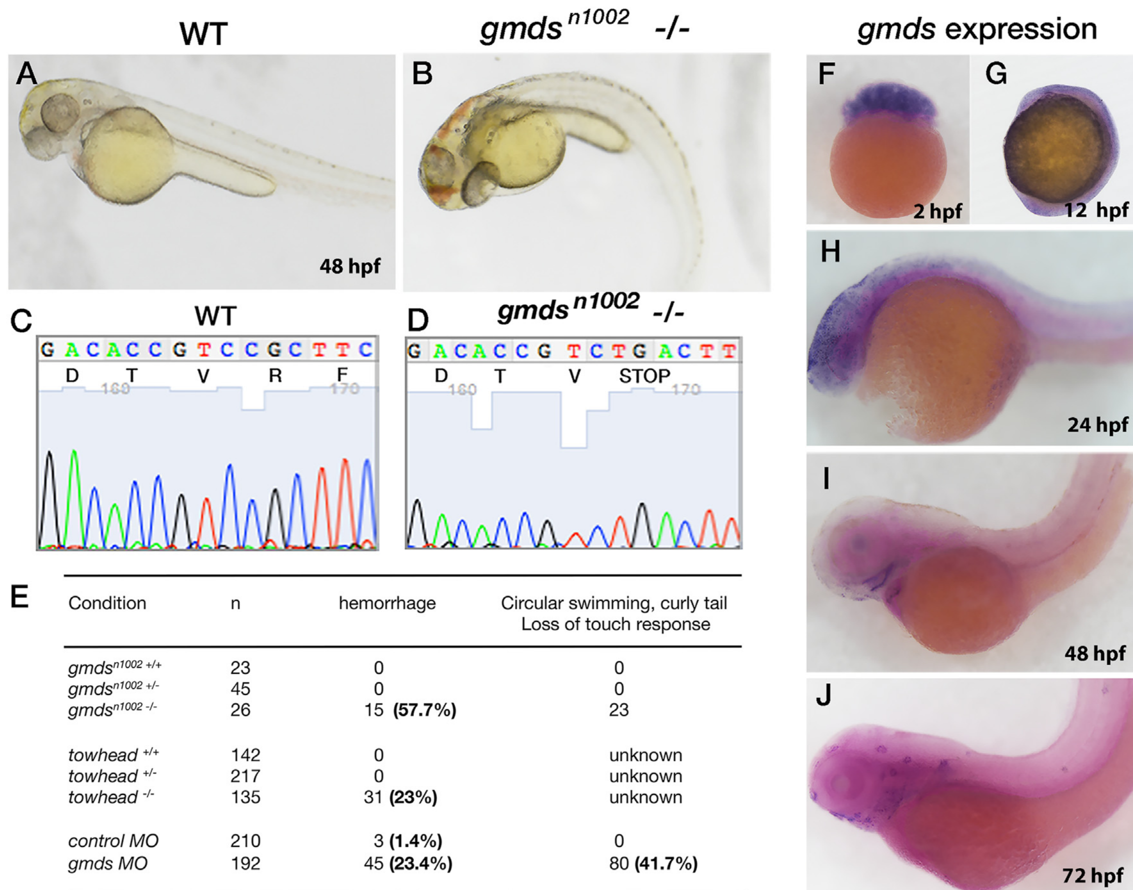


| Condition | n | hemorrhage | Circular swimming, curly tail Loss of touch response |
|---|---|---|---|
| $gmds^{n1002\ +/+}$ | 23 | 0 | 0 |
| $gmds^{n1002\ +/-}$ | 45 | 0 | 0 |
| $gmds^{n1002\ -/-}$ | 26 | 15 **(57.7%)** | 23 |
| $towhead^{+/+}$ | 142 | 0 | unknown |
| $towhead^{+/-}$ | 217 | 0 | unknown |
| $towhead^{-/-}$ | 135 | 31 **(23%)** | unknown |
| control MO | 210 | 3 **(1.4%)** | 0 |
| gmds MO | 192 | 45 **(23.4%)** | 80 **(41.7%)** |

**Fig. 1.** Expression of *gmds* and phenotypic quantification of mutants and morphants. (A) A wildtype (WT) embryo at 48 hpf (B) A $gmd^{\ n1002\ -/-}$ mutant embryo at 48 hpf with a curly tail and cerebral hemorrhage. A sequencing chromatogram is shown from a wildtype embryo comparing a non-altered *gmds* sequence (C) to a mutant sequence (D) highlighting a missense mutation and a one base insertion at the CRISPR cut site, creating a premature ‘stop’ codon in the protein coding sequence. The rates of hemorrhage, curly tail and swimming behavior recorded at 3 dpf for $gmds^{n1002-/-}$, $gmds^{towhead-/-}$, and *gmds* morphants (E). The *gmds* gene is maternally deposited and ubiquitously expressed at 2 hpf (F). Low levels of ubiquitous expression are observed at 12 hpf (G), with expression increasing in the epidermis by 24 hpf (H). At 48 hpf, *gmds* expression is seen in the pharyngeal arches and a thin stripe in the heart (I). By 72 hpf, the pharyngeal arches and sensory neuromasts have *gmds* expression staining (J).

dpf, the hemorrhage frequency in homozygous mutants was highly penetrant at a rate of 57.7 % (Fig. 1E) based on genotyping to two pair-wise crosses. Hemorrhages are often seen (23/30 of hemorrhaging embryos based on two pair-wise crosses) adjacent to the mid cerebral vein (MCeV) and metencephalic artery (Mta), with blood accumulating in hindbrain ventricle. Hemorrhages are also observed adjacent to the anterior cerebral vein [(ACeV) 16/30 hemorrhaging embryos based on two pair-wise crosses) and often observed in conjunction with hemorrhages near the MCeV and Mta (Fig. S2). Additionally, 100% of homozygotes exhibited a curled tail and irregular swimming behavior, phenotypes that are observed in previously reported *gmds* mutant strains (Ohata et al., 2009; Song et al., 2010). Homozygous mutants are not viable past 8 dpf, and similar results are observed using morpholinos directed against *gmds* (Fig. 1E, Fig. S2). We next sought to determine if hemorrhaging phenotypes were present in one of the previously published *gmds* strains containing a point mutation ($gmds^{towhead}$). Similar to our $gmds^{n1002}$ allele, homozygous *towhead* mutants displayed cerebral hemorrhages, albeit at a lower frequency than $gmds^{n1002-/-}$ (Fig. 1E, Fig. S2). The replicated phenotypes seen between two mutant strains and *gmds* morphants provides strong evidence for a novel role for *gmds* in promoting vascular integrity and is consistent with GWA data demonstrating variants within *GMDS* associating with increased stroke risk (French et al., 2014).

### 2.2. gmds is expressed in tissues important for vascular development

To determine if *gmds* is expressed in tissues relevant to vascular development, we investigated the localized expression of *gmds* using *in situ* hybridization in wildtype embryos. *in situ* hybridization using an antisense probe specific to the *gmds* mRNA highlights maternally deposited transcripts at 2 hpf, with ubiquitous expression observed at 12 hpf, and epithelial expression by 24 hpf (Fig. 1F–H). The expression of *gmds* in epithelial cells could contribute to non-cell autonomous influence of vascular development and stability in cerebral blood vessels. Expression of the *gmds* gene is observed in the pharyngeal arches at 48 hpf and 72 hpf (Fig. 1 I and J), the site where the first major arteries of the head develop (Isogai et al., 2001; Mao et al., 2019), as well a thin strip of expression in the heart. The lack of *gmds* transcripts in these domains in *gmds* mutants (Fig. S1), could also contribute to the cerebral hemorrhaging phenotype. Transcripts for *gmds* are also observed in the lateral line neuromasts, which could contribute to the mechanism of abnormal swimming behavior observed in *gmds* mutants.

### 2.3. The fucose salvage pathway can partially compensate for loss of gmds

Previous work had shown that in addition to the *de novo* synthesis pathway that requires the action of Gmds, GDP-fucose can also be produced using dietary fucose as a substrate through a salvage pathway (Dehnert et al., 2011). The presence of the salvage pathway could play a role in the reduced penetrance of phenotypes observed in $gmds^{n1002-/-}$ mutants. *in situ* hybridization for transcripts encoding two salvage pathway catalytic enzymes, *fucose kinase* (*fcsk*) and *fucose-1-phosphate guanylyltransferase* (*fpgt*), show ubiquitous expression throughout the head (Fig. 2A, C), compared to negative control sense probes (Fig. 2B, D). We hypothesized that loss of GDP-fucose through both methods combined would result in increased penetrance of vascular phenotypes. Morpholinos designed against the *fcsk* gene were injected into clutches derived from *gmds* heterozygous matings, which increased hemorrhage rates in an additive manner compared to clutches injected with negative control morpholinos (*gmds* clutch 7.9%, *fcsk* MO clutch 9.4%, *fcsk* MO in *gmds* clutch 18.4%, ($p = 0.002$ *gmds* vs *gmds/fcsk* MO, $p = 0.003$ *fcsk* MO vs *gmds/fcsk* MO) (Fig. 2E). Thus the salvage pathway likely plays a small but significant role in promoting vascular integrity, supported by the increased penetrance of hemorrhages through morpholino inhibition of *fucose kinase* in a *gmds* mutant background.

Given the ability of the salvage pathway to contribute to vascular phenotypes, we reasoned that providing embryos with L-fucose, the substrate of the salvage pathway, may rescue cerebral hemorrhaging in *gmds* mutants. This assumes that hemorrhages are the result of the loss of GDP-fucose, and not the build-up of mannose-based substrates that would presumably accumulate due to loss of *gmds*. Injections of GDP-fucose (a positive control) significantly reduces hemorrhage frequency in clutches derived from $gmds^{n1002+/-}$ incrosses (Fig. 2F). This rescue was dose dependent [10 mM GDP-fucose reduced hemorrhage rate by 61% ($p < 0.0001$), while 50 mM GDP-fucose reduced hemorrhage frequency by 74%, ($p < 0.0001$)]. This demonstrates that it is indeed the loss of GDP-fucose production that causes cerebral hemorrhage. Injection of L-fucose (salvage pathway substrate) also significantly reduces hemorrhage rate, but not as efficiently as GDP-fucose (Fig. 2F). While injection of 10 mM fucose tends to reduce hemorrhage frequency, this was not statistically significant. Clutches injected with 50 mM of L-fucose exhibit a significant rescue, reducing hemorrhage frequency by 36% ($p < 0.05$, Fig. 2F). Together, these data demonstrate that the salvage pathway can partially compensate for the loss of *de novo* GDP-fucose production and likely contributes to the reduced penetrance of the hemorrhaging phenotype observed in $gmds^{n1002-/-}$, $gmds^{towhead\ -/-}$ mutants and *gmds* morphants.

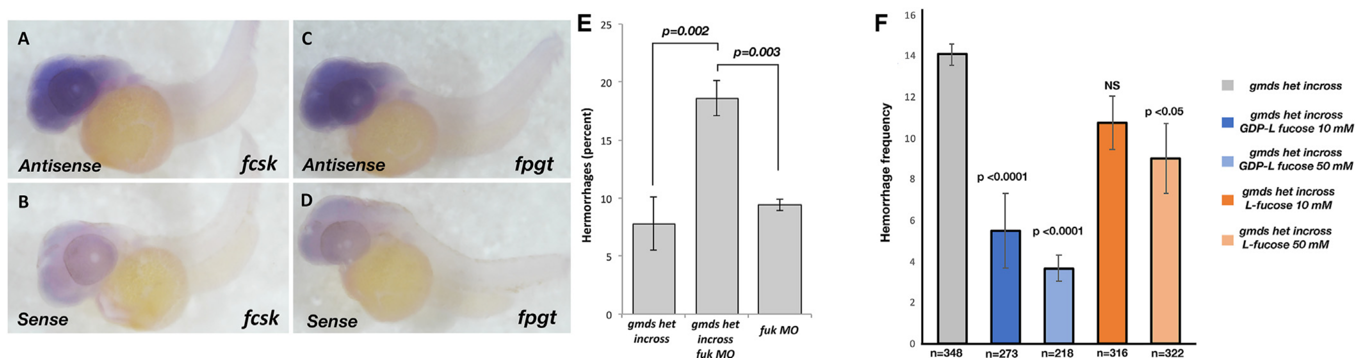


**Fig. 2.** Salvage pathway genes contribute to vascular integrity. The *fcsk* gene is expressed ubiquitously in the head of wildtype 48 hpf embryos (A) compared to the mild background staining in the wildtype control embryos using a sense probe (B). The *fpgt* gene was expressed ubiquitously in the head of wildtype 48 hpf embryos (C) compared to the mild background staining in the wildtype control embryos using a sense probe (D). The recorded cerebral hemorrhaging rates of embryo clutches derived from *gmds* heterozygous matings and control wildtype crosses with or without *fcsk* morpholino (E), showing that the *fcsk* morpholino increase hemorrhage rates. (F), results of rescue experiments using GDP-fucose and L-fucose, demonstrating that both conditions can rescue hemorrhage rate. Statistical significance was calculated using a chi-squared test with Yate's correction. Error bars represent standard error of the mean hemorrhage rate from three independent experiments.

### 2.4. Aberrant Notch signaling contributes to the hemorrhage phenotype in gmds mutants

Notch receptors play key roles in vascular development and can activate or inhibit vessel formation and maturation depending on specific ligand receptor interactions (Antfolk et al., 2017; Hofmann and Iruela-Arispe, 2007). EGF-like repeats on the extracellular domain of Notch receptors are fucosylated by the Fringe family of glycosyltransferases (Kakuda and Haltiwanger, 2017; Pandey et al., 2019; Yamakawa et al., 2012), which is thought to regulate receptor-ligand interactions and provides a pathway for vascular dysfunction in *gmds* mutant embryos. We thus assessed whether inhibiting or activating Notch signaling could affect hemorrhage rates in mutant clutches derived from *gmds* heterozygous matings. Given the hemorrhage phenotypes is not fully penetrant, we reasoned that suboptimal inhibition of Notch signaling in clutches derived from *gmds* heterozygous mutant crosses would increase hemorrhage rate. Incubation of clutches in a low dose of DAPT (which inhibits Gamma Secretase that is required for cleavage of the Notch intracellular domain) cause a low level of hemorrhage in wildtype embryos and a synergistic increase in hemorrhage rates in *gmds* mutants (Fig. 3A). Incubation in 10 mM DAPT causes a hemorrhage rate of 5.5% in wildtype clutches and the same dose of DAPT increases hemorrhage rate from 14.2% to 31.8 % ($p = 0.0035$) in clutches derived from heterozygous mutant parents, supporting the hypothesis that hemorrhages in *gmds* mutants are at least partially dependent of Notch signaling.

A role for Notch signaling downstream of *gmds* would predict that increasing Notch signaling in a *gmds* mutant a background would reduce hemorrhage frequency. We tested whether increasing Notch signaling through overexpression of the Notch Intracellular Domain (NICD) could rescue hemorrhage frequency in *gmds* mutants, as supplying *NICD* mRNA should bypass the requirement of receptor fucosylation and ligand binding. Injection of *NICD mRNA* into one cell zebrafish embryos reduces hemorrhage frequency in clutches derived from heterozygous parents in a dose dependent manner. At a low dose (50 pg per embryo) a trend of reduced hemorrhage frequency is observed but is not statistically significant. At the 100 pg dose, a significant reduction of hemorrhage frequency is observed [$12.2 \pm 1.6$ for injected clutches vs $19.5\% \pm 1.1$ for un-injected clutches ($p = 0.036$)] (Fig. 3B), supporting a role for aberrant Notch signaling as a key facet of the hemorrhage phenotypes in *gmds* mutants. While not directly tested in this study, these data imply that altered signalling potentially through dysregulation of ligand affinity for specific Notch receptors may drive the cerebral hemorrhage phenotype in *gmds* mutants.

### 2.5. gmds mutants display ectopic cerebral vessel branches and reduced mural cell coverage

Notch signaling can affect vascular development thorough defects in arterial-venous specification of endothelial cells (Lawson et al., 2001), by negatively regulating angiogenesis (Akil et al., 2021; Siekmann and Lawson, 2007), or through reduced proliferation of mural cell progenitors (Wang et al., 2014). In order understand the mechanism whereby loss of *gmds* results in cerebral hemorrhage, we imaged endothelial and mural cell markers to assess potential defects. Analysis of *gfp* driven by the *fli1a* (endothelial) promoter demonstrates that *gmds* homozygous mutants have ectopic endothelial cell branches and connections at both 2 dpf (Fig. S3 A, B) and 3 dpf (Fig. 4 A-E), corresponding to the developmental time points where cerebral hemorrhages are observed. These data are consistent with the reduced Notch signalling in *gmds* mutants and the known role of this pathway in negatively regulating angiogenesis. No difference in endothelial cell marker expression including *kdrl*, *pecam1*, and *cldn5b* are observed at these time points (Fig. S3 C–H), and thus endothelial cell specification and the formation of tight junctions likely do not influence this phenotype. Given the known role of Notch signalling is specifying arterial endothelial cell identity (Lawson et al., 2001), we tested whether arterial-venous specification of endothelial cells is altered due to loss of *gmds*. While *notch* mutants

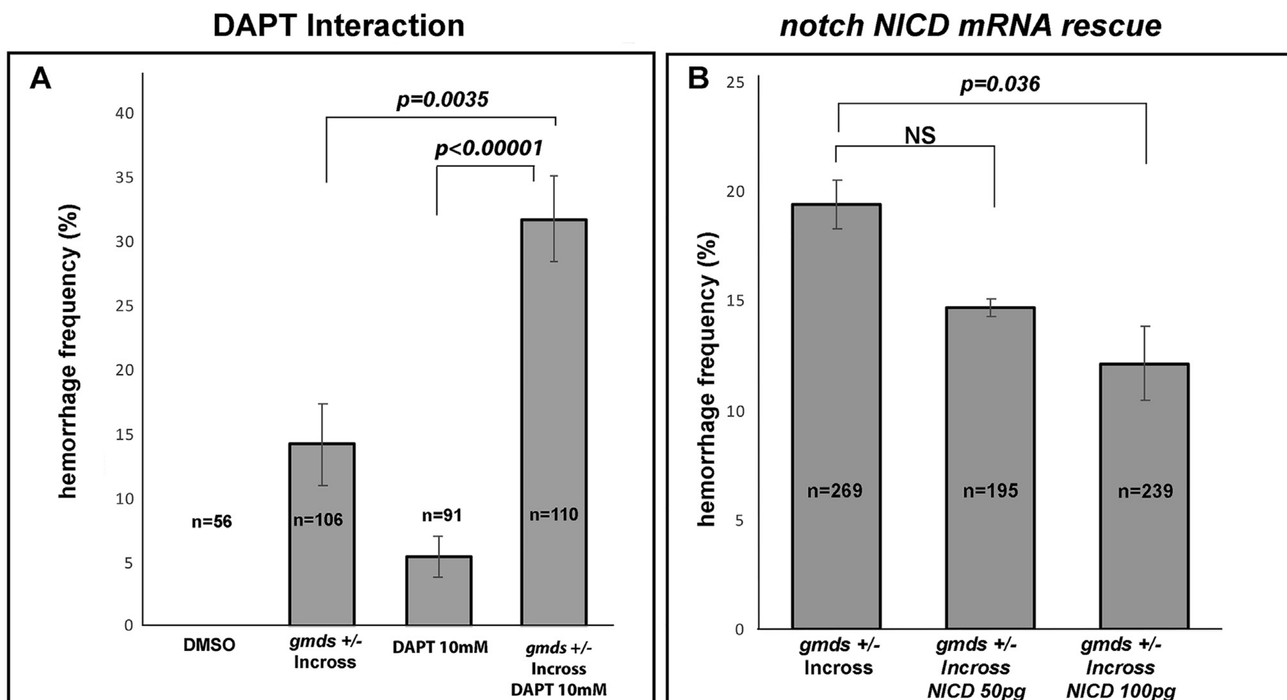


**Fig. 3.** Manipulation of Notch signaling affects hemorrhage rates in *gmds* mutant embryos. A synergistic increase in hemorrhage frequency is observed when clutches of embryos derived from *gmds* heterozygous matings are incubated in a low dose of DAPT (A). Overexpression of the Notch intracellular domain rescues (reduces) hemorrhage frequency in clutches derived from *gmds* heterozygous matings (B). Hemorrhages were quantified at 50 hpf, Chi-squared analysis with Yate's correction was used for statistical testing. Data presented as mean hemorrhage frequency across three independent experiments with error bars representing standard error of the mean.

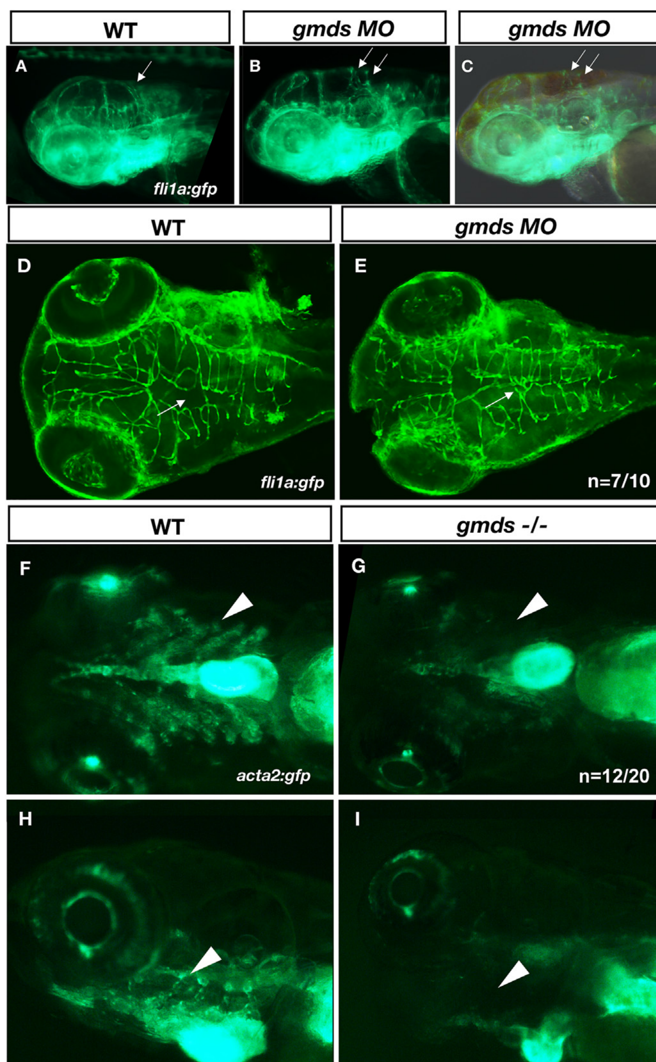


**Fig. 4.** Analysis of endothelial cell organization and smooth muscle cell number due to loss of *gmds*. In *gmds* morphant embryos, ectopic branches of cerebral vessels are observed at 3 dpf (B, C, E white arrows) when compared to control injected embryos (A, D). Panel C shows merged *gfp* and brightfield images to show the location of cerebral hemorrhage (hindbrain ventricle) near the site of an ectopic branch as highlighted by *fli1a:gfp* expression. *gmds* mutant embryos showed decreased smooth muscle actin cells in the bulbus arteriosus and pharyngeal arch arteries (G ventral view, I, lateral view) compared to wildype siblings (F, ventral view, H, lateral view) at 5 dpf. Embryos were deemed wildtype (+/+ or +/−) based on a lack of hemorrhage and curly tail, or mutant based on the presence cerebral hemorrhage and curly tail.

display decreased expression of the arterial markers such as *efnb2a* and increased expression of the venous endothelial markers *ephb4* and *flt4* (Lawson et al., 2001; Lawson and Weinstein, 2002), we observe no difference in the expression of *efnb2a* in the dorsal aorta, nor any change in expression of *ephb4* and *flt4* in the ventral cardinal vein or mid-cerebral vein (the site of the majority of cerebral hemorrhages) due to loss of *gmds* function (Fig. S4 A-H).

We next assessed the number of mural cells that are recruited to developing vasculature, given that endothelial-mural cell communication is essential for vascular stability (Armulik et al., 2005). Homozygous mutants have a clear reduction in the number of smooth muscle cells lining the pharyngeal arch arteries as shown through *gfp* driven by the *acta2* promoter (Whitesell et al., 2019) (Fig. 4F–I). Reduced expression of this transgene is also observed in the bulbus arteriosus (BA) (Fig. 4A–D). *Acta2* encodes a smooth muscle actin protein and defects in this gene have been linked to a number of vascular diseases including stroke (Guo et al., 2009). Additionally, reduced expression of the smooth muscle cell marker *transgelin* (*tagln*) is observed in the heart and BA at this time (Fig. S5 A, B), reiterating the role of *gmds* in regulating markers of smooth muscle cell development. While the lack of *acta2 gfp* positive cells, and reduced expression of *tagln* could certainly contribute to the hemorrhage phenotype, both are late markers of terminally differentiated smooth muscle cells, and differences in their expression are observed after cerebral hemorrhages have occurred. Previous studies have identified mural cell association with vasculature as early as 2 dpf (Ando et al., 2016; Bahrami and Childs, 2018; Whitesell et al., 2019), before the onset of *acta2* and *tagln* expression and as such, we tested the expression of early mural cell markers to determine if defects are observed at the time of hemorrhage.

Mutation or inhibition of forkhead transcription factors (*foxc1a* and *foxc1b*) can result in cerebral hemorrhage at 48 hpf (French et al., 2014), are required for smooth muscle cell differentiation (Siegenthaler et al., 2013; Whitesell et al., 2019), and are expressed in head and cerebral vessels at 48 hpf. Moreover, eQTL analysis using publicly available data sets (Westra et al., 2013) demonstrates that the SNPs within *gmds* that are associated with stroke risk also associate with transcript levels of both *GMDS* and *FOXC1* (Table S1), implying there could be a regulatory relationship between the two genes or gene products. We therefore tested the expression of *foxc1b* and a downstream growth factor receptor (*pdgfrb*) (French et al., 2014; Siegenthaler et al., 2013) to determine if early mural cell markers are disrupted in *gmds* mutants. Expression of *foxc1b* and *pdgfrb* are unaltered in the head and cerebral vessels in *gmds* mutant embryos at 48 hpf (Fig. S5 C-F), indicating that the subsequent lack of smooth muscle cells likely isn't the result of early dysregulation of genes required for their specification. It is possible that smooth muscle cells associate with vasculature and subsequently die due to defects in protein fucosylation. Defects in Notch signalling have been shown to induce apoptosis in smooth muscle cells (Harrison et al., 2019) and while cerebral hemorrhages in *gmds* mutants are at least partially Notch dependent, survival of smooth muscle cells have not been tested as part of this study.

Our results demonstrate that ectopic branches of endothelial cells during early vessel development occur due to loss of *gmds* and likely comprise a key facet of the mechanism leading to cerebral hemorrhage. As defects in smooth muscle cell populations are observed after the cerebral hemorrhages, they may represent a secondary phenotype resulting from defects in endothelial cells or from the hemorrhage itself. However, mural cells associate with cerebral vasculature as early as 2 dpf before the onset of *acta2* and *tagln* expression, and thus it is possible that mural cell defects contribute to the increased risk of hemorrhage before detection by these markers is possible.

## 3. Conclusion

Our results support the novel hypothesis that *gmds* plays a role in vascular development and integrity as cerebral hemorrhages are observed in mutant and morphant embryos. The rescue of hemorrhage frequency through activation of Notch signalling highlights a key role for this pathway in maintaining vascular integrity downstream of *gmds*, however further work is required to determine which ligands and receptors specifically are involved. Additional work will also be required to determine if other signalling pathways that require fucosylation, such as the Wnt signalling pathway (Feng et al., 2014) play a role in maintaining vascular integrity downstream of *gmds*. While mutation of *gmds* does not affect markers of endothelial cell specification, ectopic branches are formed in the cerebral vasculature that could influence cerebral hemorrhage risk. A lack of smooth muscle cells in *gmds* mutants demonstrates a defect in vascular maturation, however whether this contributes to hemorrhage risk or represents a secondary defect after hemorrhage have occurred, remains to be determined. Lastly, our demonstration of the functionality of the fucose salvage pathway represents a potential

therapeutic avenue to overcome the pleiotropic defects observed due to loss of *gmds*, a finding with wide reaching implications given the role this gene may play in stroke risk (French et al., 2014), cancer progression (Nakayama et al., 2013), and glaucoma (Gharahkhani et al., 2014).

## 4. Materials and methods

### 4.1. Zebrafish husbandry

All experiments were performed in compliance with the standards set by the Memorial University of Newfoundland's Animal Care Committee and the Canadian Council on Animal Care. Adult zebrafish (*Danio rerio*, background strain AB) were maintained in a recirculation housing system under standard conditions and a light/dark cycle of 13:11 h. Newly fertilized embryos were collected, raised at 28.5°C and staged accordingly (Kimmel et al., 1995).

### 4.2. Generation of $gmds^{n1002}$ mutants

The CRISPR/Cas9 system was used to establish a *gmds* mutant line by designing two guide RNAs (gRNAs) targeting exon 6 of *gmds* and cloning them into the pDR274 expression vector (Hwang et al., 2013). Microinjections of two gRNA (6.2 ng/$\mu$l and 27.4 ng/$\mu$l) and nuclear localized Cas9 protein (350 ng/$\mu$l) were injected into the one cell stage of strain AB zebrafish embryos. Exon 6 of the principal *gmds* transcript was targeted using the following gRNAs: 5′-TAGGTTGGAACCCTTCGGCTGC-3′, 5′-TAGGAGGCCTGGTAGAAGCGGA-3'. The F0 injected fish were grown to three months of age and outcrossed with wildtype fish to establish heterozygous F1 founders. Sanger Sequencing of F1 founders revealed a number of alleles, with a 1 base pair insertion (bpi) used to generate the mutant population and used for all subsequent experiments. The 1 bpi mutation was accompanied by a missense mutation that creates a premature stop codon at the mutation site (Fig. 1D). This line is designated $gmds^{n1002}$ and was used for all experiments unless otherwise noted.

### 4.3. Genotyping of pairwise crosses

To genotype embryos from two pairwise crosses of $gmds^{n1002}$ heterozygotes, DNA was isolated using 50 $\mu$l 50 mM NaOH and neutralized with 5 $\mu$l 1M Tris-HCl. The *gmds* amplicon was amplified using primers (5′-CTGCATTGCTTATGTTACCGGG-3′, 5′-AATGCGTATGTTTGCTGACCAT-3′), followed by Sanger sequencing. To genotype the embryos for four $gmds^{towhead}$ heterozygous matings, the *islet 1:gfp* transgene was used to detect fully penetrant aberrant migration of vagus motor neuron progenitors (Ohata et al., 2009).

### 4.4. Morpholino and sugar injections

Morpholino antisense oligonucleotides targeting the intron-exon junction of *gmds* (CGTATGTTTGCTGACCATAAGGCGA, Gene Tools) and *fcsk* (TGTATAAAAGTTGCTCACCCTGTCG, Gene Tools) were injected into the one cell stage of *gmds* mutant and wildtype embryos to knockdown the function of these genes. A standard oligonucleotide, with no specific target, (CCTCTTACCTCAGTTACAATTTATA, Gene Tools) was injected to act as a negative injection control. A p53 targeted (GCGCCATTGCTTTGCAAGAATTG, Gene Tools) morpholino was also coinjected with *fcsk* morpholinos to circumvent cell death. For injection of GDP-Fucose and L-fucose, stock sugars were purchased from Sigma -Aldrich, dissolved in water to the desired concentration and injected directly into the yolk sac of one-cell embryos. Significance was calculated using chi-squared analysis with Yate's correction.

### 4.5. Probe design and in situ hybridization

A T7 RNA polymerase promoter sequence (5′ TAATACGACTCACTATAGGG 3′) was added to the 5′ end of the reverse primer to allow for downstream antisense probe synthesis, or to the 5' end of the forward primer to generate sense (negative control) probes. Probes were synthesized from the cDNA using a protocol modified from Thisse and Thisse (Thisse and Thisse (2008). Primer sequences for each *in situ* hybridization probe are listed in Table S2. Embryos intended for *in situ* hybridization were grown in 0.003% 1-phenyl 2-thiourea (PTU; Sigma-Aldrich) to prevent pigment formation. The 24 hpf, 48 hpf, and 72 hpf embryos were permeabilized using *proteinase k* for 3 min, 15 min, and 30 min, respectively. NBT/BCIP or BM purple (Sigma-Aldrich) was used for coloration.

### 4.6. DAPT treatments

(2S)–N-[(3,5-Difluorophenyl)acetyl]-L-alanyl-2-phenyl]glycine 1,1-dimethylethyl ester (DAPT) was used to inhibit Notch Signaling at a concentration of 10 mM (dissolved in DMSO) in clutches derived from heterozygous incrosses. DAPT was added to embryos at 22 hpf, with hemorrhages being quantified at 48 hpf. An equal amount of DMSO was added to separate clutches as a control. For hemorrhage quantification, researchers were blinded to treatment. Significance was calculated using chi-squared analysis with Yate's correction.

### 4.7. NICD injection

The *notch intracellular domain mRNA* (eGFP tagged) was synthesized from (pCSegfpN5ICD) (Villefranc et al., 2007). The vector was linearized with (NotI) and sense RNA was transcribed via the SP6 promoter using an mMessage Machine kit (Thermo Fisher). Injection of 50 pg of mRNA resulted in normal appearing embryos, while a small fraction of embryos injected with 100 pg of mRNA exhibited mild defects including curled tails and altered somite boundaries, however cerebral vasculature appeared normal and blood flow was established, thus these embryos were included in analyses. Injection of 200 pg or higher resulted in more severe defects, often with vascular and blood flow abnormalities, and thus analyses were limited to 50 pg and 100 pg injections. Significance was calculated using chi-squared analysis with Yate's correction. Visualization of *egfp* expression was utilized to ensure proper mRNA injection and translation into protein (Fig. S6).

## Summary statement

This study identifies a novel role for the protein fucosylation pathway in blood vessel development and stroke risk.

## Declaration of competing interest

None of the authors have any conflicts of interest to disclose.


## Acknowledgments

We would like to thank Dr. Sarah Childs (University of Calgary) for providing the *acta2:gfp* line, the Dalhousie University Zebrafish Core for providing the *fli1a:gfp* line, and the animal care staff at Memorial University and Riken for fish care. Funding for this work was provided by the Natural Sciences and Research Council of Canada (NSERC), Memorial University (Dean's support Fund), and the Japan Society for the Promotion of Science, Japan (JSPS). Gerissa Fowler was funded through the Indspire Aboriginal Scholarship, Terra Nova Aboriginal Masters Student Scholarship, and the Bursary Program of the NunatuKavut Community Council in Newfoundland and Labrador.


## Appendix A. Supplementary data

Supplementary data to this article can be found online at https://doi.org/10.1016/j.ydbio.2021.08.004.

## References


Akil, A., Gutierrez-Garcia, A.K., Guenter, R., Rose, J.B., Beck, A.W., Chen, H., Ren, B., 2021. Notch signaling in vascular endothelial cells, angiogenesis, and tumor progression: an update and prospective. Front Cell Dev Biol 9, 642352.

Ando, K., Fukuhara, S., Izumi, N., Nakajima, H., Fukui, H., Kelsh, R.N., Mochizuki, N., 2016. Clarification of mural cell coverage of vascular endothelial cells by live imaging of zebrafish. Development 143, 1328–1339.

Antfolk, D., Sjoqvist, M., Cheng, F., Isoniemi, K., Duran, C.L., Rivero-Muller, A., Antila, C., Niemi, R., Landor, S., Bouten, C.V.C., et al., 2017. Selective regulation of Notch ligands during angiogenesis is mediated by vimentin. Proc. Natl. Acad. Sci. U. S. A. 114, E4574–E4581.

Armulik, A., Abramsson, A., Betsholtz, C., 2005. Endothelial/pericyte interactions. Circ. Res. 97, 512–523.

Armulik, A., Genove, G., Mae, M., Nisancioglu, M.H., Wallgard, E., Niaudet, C., He, L., Norlin, J., Lindblom, P., Strittmatter, K., et al., 2010. Pericytes regulate the blood-brain barrier. Nature 468, 557–561.

Bahrami, N., Childs, S.J., 2018. Pericyte biology in zebrafish. Adv. Exp. Med. Biol. 1109, 33–51.

Cagdas, D., Yilmaz, M., Kandemir, N., Tezcan, I., Etzioni, A., Sanal, O., 2014. A novel mutation in leukocyte adhesion deficiency type II/CDGIIc. J. Clin. Immunol. 34, 1009–1014.

Cui, X.J., Zhao, A.G., Wang, X.L., 2017. Correlations of AFAP1, GMDS and PTGFR gene polymorphisms with intra-ocular pressure response to latanoprost in patients with primary open-angle glaucoma. J. Clin. Pharm. Therapeut. 42, 87–92.

Dehnert, K.W., Beahm, B.J., Huynh, T.T., Baskin, J.M., Laughlin, S.T., Wang, W., Wu, P., Amacher, S.L., Bertozzi, C.R., 2011. Metabolic labeling of fucosylated glycans in developing zebrafish. ACS Chem. Biol. 6, 547–552.

Ehling, M., Adams, S., Benedito, R., Adams, R.H., 2013. Notch controls retinal blood vessel maturation and quiescence. Development 140, 3051–3061.

Feng, L., Jiang, H., Wu, P., Marlow, F.L., 2014. Negative feedback regulation of Wnt signaling via N-linked fucosylation in zebrafish. Dev. Biol. 395, 268–286.

French, C.R., Seshadri, S., Destefano, A.L., Fornage, M., Arnold, C.R., Gage, P.J., Skarie, J.M., Dobyns, W.B., Millen, K.J., Liu, T., et al., 2014. Mutation of FOXC1 and PITX2 induces cerebral small-vessel disease. J. Clin. Invest. 124, 4877–4881.

Gaengel, K., Genove, G., Armulik, A., Betsholtz, C., 2009. Endothelial-mural cell signaling in vascular development and angiogenesis. Arterioscler. Thromb. Vasc. Biol. 29, 630–638.

Gharahkhani, P., Burdon, K.P., Fogarty, R., Sharma, S., Hewitt, A.W., Martin, S., Law, M.H., Cremin, K., Bailey, J.N.C., Loomis, S.J., et al., 2014. Common variants near ABCA1, AFAP1 and GMDS confer risk of primary open-angle glaucoma. Nat. Genet. 46, 1120–1125.

Gore, A.V., Monzo, K., Cha, Y.R., Pan, W., Weinstein, B.M., 2012. Vascular development in the zebrafish. Cold Spring Harb Perspect Med 2, a006684.

Guo, D.C., Papke, C.L., Tran-Fadulu, V., Regalado, E.S., Avidan, N., Johnson, R.J., Kim, D.H., Pannu, H., Willing, M.C., Sparks, E., et al., 2009. Mutations in smooth muscle alpha-actin (ACTA2) cause coronary artery disease, stroke, and Moyamoya disease, along with thoracic aortic disease. Am. J. Hum. Genet. 84, 617–627.

Harrison, O.J., Torrens, C., Salhiyyah, K., Modi, A., Moorjani, N., Townsend, P.A., Ohri, S.K., Cagampang, F., 2019. Defective NOTCH signalling drives smooth muscle cell death and differentiation in bicuspid aortic valve aortopathy. Eur. J. Cardio. Thorac. Surg. 56, 117–125.

Hellberg, C., Ostman, A., Heldin, C.H., 2010. PDGF and vessel maturation. Recent Results Canc. Res. 180, 103–114.

Hofmann, J.J., Iruela-Arispe, M.L., 2007. Notch signaling in blood vessels: who is talking to whom about what? Circ. Res. 100, 1556–1568.

Hwang, W.Y., Fu, Y., Reyon, D., Maeder, M.L., Tsai, S.Q., Sander, J.D., Peterson, R.T., Yeh, J.R., Joung, J.K., 2013. Efficient genome editing in zebrafish using a CRISPR-Cas system. Nat. Biotechnol. 31, 227–229.

Isogai, S., Horiguchi, M., Weinstein, B.M., 2001. The vascular anatomy of the developing zebrafish: an atlas of embryonic and early larval development. Dev. Biol. 230, 278–301.

Kakuda, S., Haltiwanger, R.S., 2017. Deciphering the fringe-mediated notch code: identification of activating and inhibiting sites allowing discrimination between ligands. Dev. Cell 40, 193–201.

Kimmel, C.B., Ballard, W.W., Kimmel, S.R., Ullmann, B., Schilling, T.F., 1995. Stages of embryonic development of the zebrafish. Dev. Dynam. 203, 253–310.

Lanner, F., Sohl, M., Farnebo, F., 2007. Functional arterial and venous fate is determined by graded VEGF signaling and notch status during embryonic stem cell differentiation. Arterioscler. Thromb. Vasc. Biol. 27, 487–493.

Lawson, N.D., Scheer, N., Pham, V.N., Kim, C.H., Chitnis, A.B., Campos-Ortega, J.A., Weinstein, B.M., 2001. Notch signaling is required for arterial-venous differentiation during embryonic vascular development. Development 128, 3675–3683.

Lawson, N.D., Weinstein, B.M., 2002. Arteries and veins: making a difference with zebrafish. Nat. Rev. Genet. 3, 674–682.

Mao, A., Zhang, M., Liu, J., Cao, Y., Wang, Q., 2019. PDGF signaling from pharyngeal pouches promotes arch artery morphogenesis. J Genet Genomics 46, 551–559.

Moriwaki, K., Noda, K., Furukawa, Y., Ohshima, K., Uchiyama, A., Nakagawa, T., Taniguchi, N., Daigo, Y., Nakamura, Y., Hayashi, N., et al., 2009. Deficiency of GMDS leads to escape from NK cell-mediated tumor surveillance through modulation of TRAIL signaling. Gastroenterology 137, 188–198, 198 e181-182.

Naito, H., Iba, T., Takakura, N., 2020. Mechanisms of new blood-vessel formation and proliferative heterogeneity of endothelial cells. Int. Immunol. 32, 295–305.

Nakayama, K., Moriwaki, K., Imai, T., Shinzaki, S., Kamada, Y., Murata, K., Miyoshi, E., 2013. Mutation of GDP-mannose-4,6-dehydratase in colorectal cancer metastasis. PloS One 8, e70298.

Ohata, S., Kinoshita, S., Aoki, R., Tanaka, H., Wada, H., Tsuruoka-Kinoshita, S., Tsuboi, T., Watabe, S., Okamoto, H., 2009. Neuroepithelial cells require fucosylated glycans to guide the migration of vagus motor neuron progenitors in the developing zebrafish hindbrain. Development 136, 1653–1663.

Pandey, A., Harvey, B.M., Lopez, M.F., Ito, A., Haltiwanger, R.S., Jafar-Nejad, H., 2019. Glycosylation of specific notch EGF repeats by O-Fut1 and Fringe regulates notch signaling in Drosophila. Cell Rep. 29, 2054–2066 e2056.

Scheppke, L., Murphy, E.A., Zarpellon, A., Hofmann, J.J., Merkulova, A., Shields, D.J., Weis, S.M., Byzova, T.V., Ruggeri, Z.M., Iruela-Arispe, M.L., et al., 2012. Notch promotes vascular maturation by inducing integrin-mediated smooth muscle cell adhesion to the endothelial basement membrane. Blood 119, 2149–2158.

Siegenthaler, J.A., Choe, Y., Patterson, K.P., Hsieh, I., Li, D., Jaminet, S.C., Daneman, R., Kume, T., Huang, E.J., Pleasure, S.J., 2013. Foxc1 is required by pericytes during fetal brain angiogenesis. Biol Open 2, 647–659.

Siekmann, A.F., Lawson, N.D., 2007. Notch signalling limits angiogenic cell behaviour in developing zebrafish arteries. Nature 445, 781–784.

Song, Y., Willer, J.R., Scherer, P.C., Panzer, J.A., Kugath, A., Skordalakes, E., Gregg, R.G., Willer, G.B., Balice-Gordon, R.J., 2010. Neural and synaptic defects in slytherin, a zebrafish model for human congenital disorders of glycosylation. PloS One 5, e13743.

Sturla, L., Fruscione, F., Noda, K., Miyoshi, E., Taniguchi, N., Contini, P., Tonetti, M., 2005. Core fucosylation of N-linked glycans in leukocyte adhesion deficiency/congenital disorder of glycosylation IIc fibroblasts. Glycobiology 15, 924–934.

Sturla, L., Rampal, R., Haltiwanger, R.S., Fruscione, F., Etzioni, A., Tonetti, M., 2003. Differential terminal fucosylation of N-linked glycans versus protein O-fucosylation in leukocyte adhesion deficiency type II (CDG IIc). J. Biol. Chem. 278, 26727–26733.

Takeuchi, H., Haltiwanger, R.S., 2014. Significance of glycosylation in Notch signaling. Biochem. Biophys. Res. Commun. 453, 235–242.

Thisse, C., Thisse, B., 2008. High-resolution in situ hybridization to whole-mount zebrafish embryos. Nat. Protoc. 3, 59–69.

Villefranc, J.A., Amigo, J., Lawson, N.D., 2007. Gateway compatible vectors for analysis of gene function in the zebrafish. Dev. Dynam. 236, 3077–3087.

Wang, Y., Huang, D., Chen, K.Y., Cui, M., Wang, W., Huang, X., Awadellah, A., Li, Q., Friedman, A., Xin, W.W., et al., 2017. Fucosylation deficiency in mice leads to colitis and adenocarcinoma. Gastroenterology 152, 193–205 e110.

Wang, Y., Pan, L., Moens, C.B., Appel, B., 2014. Notch 3 establishes brain vascular integrity by regulating pericyte number. Development 141, 307–317.

Westra, H.-J., Peters, M.J., Esko, T., Yaghootkar, H., Schurmann, C., Kettunen, J., Christiansen, M.W., Fairfax, B.P., Schramm, K., Powell, J.E., et al., 2013. Systematic identification of trans eQTLs as putative drivers of known disease associations. Nat. Genet. 45, 1238–1243.

Whitesell, T.R., Chrystal, P.W., Ryu, J.R., Munsie, N., Grosse, A., French, C.R., Workentine, M.L., Li, R., Zhu, L.J., Waskiewicz, A., et al., 2019. foxc1 is required for embryonic head vascular smooth muscle differentiation in zebrafish. Dev. Biol. 453, 34–47.

Yamakawa, T., Ayukawa, T., Matsuno, K., 2012. Metabolism and transportation pathways of GDP-fucose that are required for the O-fucosylation of Notch. Adv. Exp. Med. Biol. 727, 37–46.

Zhou, L., Li, L.W., Yan, Q., Petryniak, B., Man, Y., Su, C., Shim, J., Chervin, S., Lowe, J.B., 2008. Notch-dependent control of myelopoiesis is regulated by fucosylation. Blood 112, 308–319.